

# Unsupervised edge map scoring: a statistical complexity approach.

Javier Gimenez<sup>a</sup>, Jorge Martinez<sup>b</sup>, Ana Georgina Flesia<sup>a</sup>

<sup>a</sup>*Facultad de Matemática, Astronomía y Física, Universidad Nacional de Córdoba. Ing. Medina Allende s/n, Ciudad Universitaria CP 5000, Córdoba, Argentina.*

<sup>b</sup>*Departamento de Matemática, Universidad Nacional del Sur, Avenida Alem 1253. 2do Piso Bahía Blanca, B8000CPB, Argentina.*

---

## Abstract

We propose a new Statistical Complexity Measure (SCM) to qualify edge maps without Ground Truth (GT) knowledge. The measure is the product of two indices, an *Equilibrium* index  $\mathcal{E}$  obtained by projecting the edge map into a family of edge patterns, and an *Entropy* index  $\mathcal{H}$ , defined as a function of the Kolmogorov Smirnov (KS) statistic.

This new measure can be used for performance characterization which includes: (i) the specific evaluation of an algorithm (intra-technique process) in order to identify its best parameters, and (ii) the comparison of different algorithms (inter-technique process) in order to classify them according to their quality.

Results made over images of the South Florida and Berkeley databases show that our approach significantly improves over Pratt's Figure of Merit (PFoM) which is the objective reference-based edge map evaluation standard, as it takes into account more features in its evaluation.

*Keywords:* unsupervised quality measure, edge maps, statistical complexity, edge patterns, entropy, Kolmogorov Smirnov statistic

---

## 1. Introduction

In most image processing techniques, the detection and handling of the edge structure of the input image is very important. From object detection to image transmission, the quality of edge manipulation takes great part in the success of the processing. Nevertheless, there is no universal definition of the notion of edge. For Abdou and Pratt, an edge is defined as a local change in luminance or discontinuity in the luminance intensity of the image [1] while Kitchen and Rosenfeld pointed out that the edge concept depends on the type of processing and analysis in which it is involved [2].

Therefore, many researchers have designed optimal Edge Detection Algorithms (EDA) related to different properties of the edge structure, but only a few have studied how to measure the edge strength and quality of general edge maps [3]. Effective and objective Edge Detection (ED) evaluation measures must be developed in order to assess EDA performance.

---

*Email addresses:* [jgimenez@mate.uncor.edu](mailto:jgimenez@mate.uncor.edu) (Javier Gimenez), [martinez@uns.edu.ar](mailto:martinez@uns.edu.ar) (Jorge Martinez), [flesia@famaf.unc.edu.ar](mailto:flesia@famaf.unc.edu.ar) (Ana Georgina Flesia)

In general, ED evaluation measures can be classified due to the need of a reference map called Ground Truth (GT) (supervised or unsupervised measures) and the type of score that they output, quantitative or qualitative. Some well known examples of quantitative supervised measures, also called discrepancy measures, are Pratt’s Figure of Merit (PFoM) [4], Kappa index [5], and Baddeley’s Delta Metric (BDM) [6]. A comparison between these discrepancy measures and some other supervised statistical measures were performed in [7]. Two main conclusions were drawn from their experiments: i) up to date, there is no convincing solution for edge image comparison or quality evaluation; ii) the biases of the measures can be helpful in applications where there is a particular interest in penalizing or ignoring some specific kind of error. A supervised quality metric for binary documents based on structural pixel matching, taking into account global edge structures introducing a smoothness term in the matching function was proposed in [8]. Examples of binary documents are text files either photocopied, faxed or scanned, with fast publishing resolution. In this kind of binary documents, bad visual word understanding is not always related to classical low scoring. PFoM is known to give high scores to lighter maps, with high rate of false negatives, but it is not acquiescent to human perception [9].

Without the guide of a GT, assessing edge maps quality is a more difficult task. The unsupervised ED measures that are found in the literature look for specific characteristics of the input edge map, such as coherence, [10], continuity, [2], smoothness and good continuation, [11, 12], or an specific pattern identification, [13], among others [14, 15]. Bower et al. studied the bias introduced by the search of only one characteristic [16]. They reported a similar conclusion to the one given by [7]: there is no unique solution; moreover, selected best maps are qualitatively different, and bias can not be estimated without further assumption of the error incurred.

Recently, Yitzhaky and Peli proposed an unsupervised evaluation procedure of ED techniques based on the consensus approach [17]. Using the correspondence between different standard EDA results, an estimated best edge map (*consensus map*) was obtained and later used as an estimated ground truth (EGT). Correspondence was computed by using both a receiver operating characteristics (ROC) analysis and a Chi-square test for standard binary outputs, considering a trade off between structure and noisiness in the detection results. Fernandez-Garcia et al. provided a definition of *consensus edge map* that is close to the notion of confidence set. They argued that in order to compare ED procedures, it is not esencial to use the best and exact GT; rather it is only necessary to use a reliable EGT that allows correct classification or ranking of the EDA to be obtained, [18]. They also noted that their approach may be used to evaluate detections from different EDA (inter-technique performance characterization) only if these detectors aim at the same output format. Our proposed evaluation methods also take into account this assumption.

The consensus approach suffers from bias regarding the generation of the candidate edge maps used to define the EGT. If the majority of the edge maps considered are not of adequate quality or fail to extract certain edge structures which are detected by only a small selection of the edge maps, this will be reflected both in the consensus EGT and in the quality of the evaluation methodology derived from it. In a sense, it penalizes algorithms that do not agree with the failures of the other algorithms.

In this paper we define a new non-reference measure that does not depend, directly or indirectly, on GT data. As the previous measures, it can be used for ED performance char-

acterization which includes: (i) the specific evaluation of an algorithm (intra-technique process) in order to identify its best parameters, and (ii) the comparison of different algorithms with the same output format (inter-technique process) in order to classify them according to their quality.

Our proposal, denoted Statistical Complexity Measure (SCM) searches for a compromise between two extreme values in the space of edge maps: a map with few edge points in a perfect shape (*Equilibrium*) and with many edge points randomly located (*Information*). The new measure is the product of two indices, an *Equilibrium* index  $\mathcal{E}$  obtained by combining local correlation between the edge map and a family of predetermined edge patterns and an *Entropy* index  $\mathcal{H}$ , defined as a function of the Kolmogorov Smirnov (KS) statistic. SCM gives value between zero and one, being zero the minimum and one the maximum quality.

Konishi et al. defined an statistical ED algorithm which relies on Chernoff information and entropy of probability distributions conditional to edge and non-edge state [15]. Their validation experiments studied elements similar to the indices that are part of our Complexity Measure. They also noted that maps with scattered random points may give high information regardless the real structure of the image, but the combinations of shape seeking measures with entropy functionals greatly reduces the probability of such anomalies.

The paper is organized as follows. In Section 2, a cosine based discrepancy measure  $\mathcal{Q}_{\mathfrak{B}}$  to score a map against a collection of hand-made GT (supervised case), or against a collection of fixed significant patterns (unsupervised case) is introduced. In Section 3 the concepts behind the *Equilibrium* index  $\mathcal{E}$  and *Entropy* index  $\mathcal{H}$  are introduced, and the final SCM  $\mathcal{C}$  as the product of both indices is defined. Experiments and results are discussed in Section 4 and conclusions and comments are left for Section 5.

## 2. Cosine-based Similarity Measure (CSM).

In this section, a cosine-based similarity measure  $\mathcal{Q}_{\mathfrak{B}}$  is introduced as an intermediate step in the definition of the final measure  $\mathcal{C}$ , along with necessary notation. Let  $I$  be an

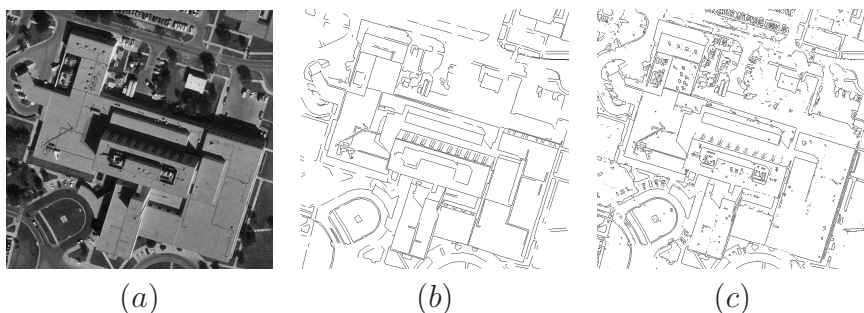


Figure 1: Evaluation of CSM (a) Original *Large Building* image from South Florida database , (b) GT, (c) Sobel ED output (thresholding parameter  $T = 0.068$ ) with  $\mathcal{Q}_{\mathfrak{B}} = 0.3976$ .

image,  $\mathbf{b}$  an edge map associated with  $I$ , (this is,  $\mathbf{b}$  is a binary image with the same size as  $I$ ), and  $\mathbf{g}$  its GT (if it is available). Figure 1 shows an example of such images. A

simple measure of similarity between  $\mathbf{b}$  and  $\mathbf{g}$  is the cosine of the angle between them [19], when they are seen as 1-D vectors (concatenating all columns one under another).

We define the index  $\mathcal{Q}_{\mathfrak{B}}$  as the maximum of all similarity values

$$\mathcal{Q}_{\mathfrak{B}}(\mathbf{b}) = \max_{1 \leq i \leq n} \mathcal{Q}(\mathbf{g}_i, \mathbf{b}) = \max_{1 \leq i \leq n} \frac{\mathbf{g}_i^T \mathbf{b}}{\|\mathbf{g}_i\| \|\mathbf{b}\|}. \quad (1)$$

being  $\|\mathbf{x}\| = \sqrt{\mathbf{x}^T \mathbf{x}}$ , and  $\mathfrak{B} = \{\mathbf{g}_1, \mathbf{g}_2, \dots, \mathbf{g}_n\}$  a collection of GT images (that could have only one element).

The Cauchy Schwartz inequality implies that the index is upper bounded by one thus attaining such bound only when the map is optimal ( $\mathbf{b} \in \mathfrak{B}$ ). Since edge maps and GT images are binary images, the index is lower bounded by 0, attained only in the absence of any similarity (when  $\mathbf{b}$  is orthogonal to  $\mathfrak{B}$ ). When no GT is available, predefined edge patterns may be locally sought in the edge map with this measure.

### 3. A statistical complexity measure (SCM)

In this section, a new SCM in the context of unsupervised evaluation of edge maps is introduced. This new measure can be used to identify the optimal parameters of a given algorithm, but also to compare and rank the results of different algorithms. In this framework, the concepts of *Equilibrium* and *Information* can be discussed and scoring indices for such qualities in edge maps can be proposed.

Following the general structure of complexity measures described by [20], SCM is defined as

$$\mathcal{C}(\mathbf{b}) = \mathcal{E}(\mathbf{b})\mathcal{H}(\mathbf{b}), \quad (2)$$

where  $\mathcal{E}$  is an *Equilibrium* index,  $\mathcal{H}$  is an *Entropy* index, and  $\mathbf{b}$  is an edge map. To define such indices, the concepts of *Equilibrium* and *Information* in the context of ED must be discussed. An edge map is well balanced (reached *Equilibrium*) if it is structurally

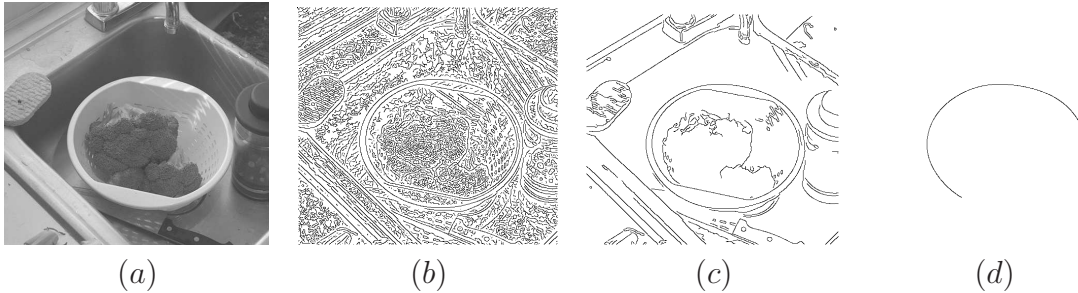


Figure 2: (a) Original 215 image from the South Florida database, (b), (c) and (d) Canny ED outputs with parameters: high threshold  $T_h = 0.01, 0.19, 0.99$ , lower threshold  $T_l = 0.4 \times T_h$ ; standard deviation  $\sigma = \sqrt{2}$ , respectively.

simple. In this sense, the map in panel (d) of Figure 2 is better balanced than the edge map in panel (c) and in turn, the one in (c) is better balanced than the one in (b). Regarding *Entropy*, one map has more information than another if the discontinuities, textures and shapes of the analyzed image are better characterized. The overabundance

of information produces chaotic (cluttered) edge maps like in (b), but the absence of information produces poor edge maps like in (d). Thus, *Equilibrium* and *Information* are two complementary concepts, and the *Complexity* searches for a balance point between them.

Thus, to quantify the *Equilibrium* of an edge map, we measured local correlation against a family of specific edge patterns assessing the correct identification and value of the usual local characteristics of edges. Since *Entropy* should measure the amount of information of a system, which is maximized when the system reaches a random state, we assess the randomness of an edge map with an index based on contrasting the statistical distribution of the spatial edge positions against the bidimensional uniform distribution.

### 3.1. Equilibrium index

Abdou and Pratt introduced in their seminal paper the notion of Figure of Merit in order to score fragmented, offset and smeared edge patterns in comparison with the ideal edges present in the GT [1]. The *Equilibrium* index should perform a similar task in the unsupervised case, thus the GT will be replaced by a family  $\mathfrak{B}$  of carefully chosen binary edge patterns.

Abusing notation, let  $\mathfrak{B} = \{\mathbf{b}_1, \mathbf{b}_2, \dots, \mathbf{b}_n\}$  be a collection of  $N \times N$  edge patterns transformed into column vectors. Sliding a  $N \times N$  window over the edge map  $\mathbf{b}$ , centered in each edge pixel position  $k$ , edge sub-maps  $\mathbf{b}_{(k)}$  are extracted and transformed into column vectors. The CSM of each sub-maps with respect to the family of edge patterns  $\mathfrak{B}$  is computed by

$$\mathcal{Q}_{\mathfrak{B}}(\mathbf{b}_{(k)}) = \max_{1 \leq j \leq n} \frac{\mathbf{b}_j^T \mathbf{b}_{(k)}}{\|\mathbf{b}_j\| \|\mathbf{b}_{(k)}\|}. \quad (3)$$

The *Equilibrium* of  $\mathbf{b}$  with respect to the family of edge patterns  $\mathfrak{B}$  is defined as the average of the local CSM computed only on edge pixels  $k$ ,

$$\mathcal{E}(\mathbf{b}) = \frac{1}{|E_{\mathbf{b}}|} \sum_{k=1}^{|E_{\mathbf{b}}|} \mathcal{Q}_{\mathfrak{B}}(\mathbf{b}_{(k)}), \quad (4)$$

where  $E_{\mathbf{b}}$  is the set of all edge pixels in the binary edge map  $\mathbf{b}$ , and  $|E_{\mathbf{b}}|$  is the cardinal number of such set.

#### 3.1.1. A family of edge patterns

The family  $\mathfrak{B}$  of edge patterns could be very general, but in this paper, as in [2], only line-like edge patterns are considered (Figure 3). Being a line segment an essential primitive graphic, it can be used to construct many other objects. Our line patterns are made with an accurate and efficient raster line-generating algorithm defined in [21]. Bresenham stated that his line algorithms provide the best-fit approximations to the true lines by minimizing the error (distance) to the true primitive. Beginning with ray traces that go through the origin, 140 edge patterns of size  $7 \times 7$  were constructed and stored in the present database (Figure 3).

In Figure 4, the values of  $\mathcal{Q}_{\mathfrak{B}}$  on different patterns that appear in a Sobel edge map (computed from image *block*) are shown. The edge pattern (c), (f), (g) and (h) show the performance of the index when the edges are close to line segments. The maps (h)-(k)

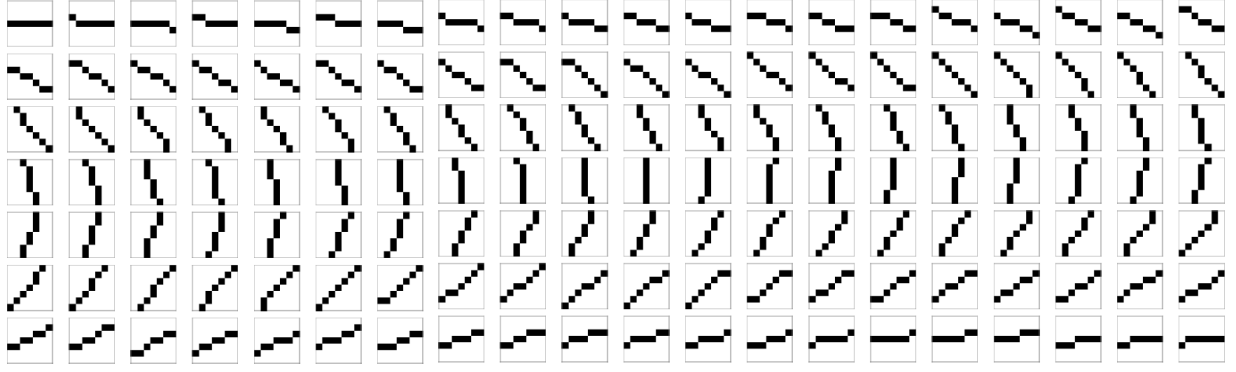


Figure 3: A family of lineal edge  $7 \times 7$  pixel patterns obtained with Bresenham's algorithm.

show the behavior of (Eq. 4) in presence of thick edges. The maximum value is reached in (h), a pattern of a line of one pixel width. Noisy patterns (b)-(e) reach an index value lower than 0.54.

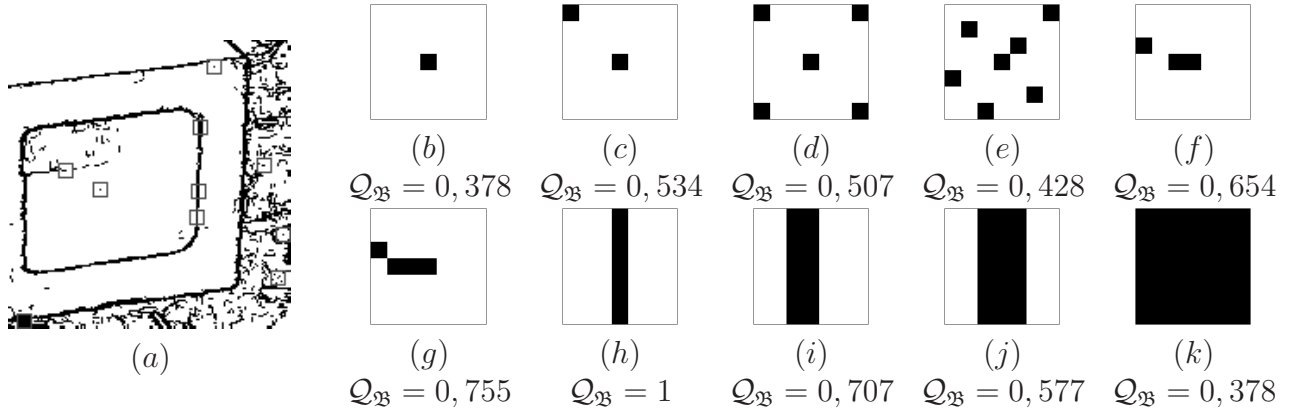


Figure 4: (a) Edge map of image *block*, (b)-(k) windows of size  $7 \times 7$  extracted from (a).

### 3.2. Information and the Kolmogorov Smirnov (KS) statistic

Shannon stated that the information provided by an observation is proportional to how improbable it was [22]. Relating this notion with the edge detection problem, having three points aligned in an edge map implies that the probability of having a fourth point next to them is higher than the probability of having a point further away. Therefore, observing a point in a place with low probability gives more information than observing a point in an expected place. Randomness in space positions is at the core of the notion of *edge information*.

Testing randomness in space is a task usually done by testing the null hypothesis of uniform distribution in the unit square with the use the KS statistic. Such statistic takes values between 0 and 1, rejecting the uniform hypothesis for values close to 1.

For a given edge map  $\mathbf{b}$ , let  $\phi = (\phi_1, \phi_2)$  be an injective function that maps the edge positions  $(i, j) \in E$  to the unit square  $[0, 1] \times [0, 1]$ , defined by  $\phi(i, j) = (\frac{2i-1}{2N}, \frac{2j-1}{2M})$  where

$N \times M$  is the image size. Let  $\mathcal{D}$  be the KS bidimensional statistic defined by

$$\mathcal{D}(\mathbf{b}) = \max_{(x,y) \in \mathbb{R}^2} |F_{\mathbf{b}}(x,y) - F(x,y)|, \quad (5)$$

where  $F$  is the cumulative distribution function of an uniform distributed bidimensional vector, and  $F_{\mathbf{b}}$  the empirical distribution function of the sample  $\phi(E)$  given by

$$F_{\mathbf{b}}(x,y) = \frac{|\{(i,j) \in E / \phi_1(i) \leq x, \phi_2(j) \leq y\}|}{|E|}. \quad (6)$$

The entropy measure  $\mathcal{H}$  is defined as

$$\mathcal{H}(\mathbf{b}) = 1 - \mathcal{D}(\mathbf{b}). \quad (7)$$

$\mathcal{D}(\mathbf{b})$  was computed using the efficient algorithm by [23].

## 4. Results and Analysis.

### 4.1. Aim of the experiments

The computational experiments shown in this section are designed to investigate both the edge discrimination power of the concepts of *Information* and *Equilibrium* implemented by  $\mathcal{H}$  and  $\mathcal{E}$  and the use of  $\mathcal{C}$  for ED performance characterization which includes: (i) the specific evaluation of an algorithm (intra-technique process) in order to identify its best parameters, and (ii) the comparison of different algorithms (inter-technique process) in order to classify them according to their quality.

In order to do so, images from benchmark databases, compiled specifically for edge detection and object boundary detection were selected, and for each image, a database of edge maps was made by sampling the parameter space of several well known gradient based ED algorithms (EDA). On such database,  $\mathcal{C}$  scoring is compared against reference-based measures, i.e. measures that take into account the GT provided by the image benchmark database.

The reference-based measures considered are our  $\mathcal{Q}_{\mathfrak{B}}$ , defined in Section 2 and the golden standard PFoM discrepancy measure given by

$$\mathcal{P}_{\alpha}(\mathbf{g}, \mathbf{b}) = \frac{1}{\max\{|E_{\mathbf{b}}|, |E_{\mathbf{g}}|\}} \sum_{k \in E_{\mathbf{b}}} \frac{1}{1 + \alpha d^2(k, E_{\mathbf{g}})},$$

where  $\alpha = 1/9$ ,  $d$  is the Euclidean measure,  $E_{\mathbf{g}}$  and  $E_{\mathbf{b}}$  are the edge pixels subset of maps  $\mathbf{g}$  and  $\mathbf{b}$  respectively, [1, 7].

The performance of  $\mathcal{C}$  in the intra technique evaluation process was done by studying the edge map selected for the maximum value of the scoring curves over the database and the actual scoring value. The former gives visual evidence and the later gives information about the balance between *Equilibrium* and *Entropy* (in the case of our unsupervised measure) and which of them is the closest to the GT in the case of PFoM and  $\mathcal{Q}_{\mathfrak{B}}$ . The scoring curves  $\mathcal{C}$ ,  $\mathcal{E}$  and  $\mathcal{H}$  also shed light on how each index reflects the degradations produced by excess or absence of edge pruning.

Several reference-based measures were compared in [7] by using a database of degraded images made by applying three different degradation operators to a single output of Canny EDA, with specific parameters selected to provide an overall good edge map related to the GT. The operators were addition of false positives, addition of false negatives, and diagonal displacements in a random fashion.

The experiments considered in this paper do not include random modifications in the map; all edges are true edges if they are considered in an appropriate scale. Also, all other EDA considered here, besides Canny, aim at the same output format as in [17, 18]. They are all gradient based EDA, thus they can be compared using quality curves [9].

Canny EDA was also used as a benchmark detector in [24]. The model presented as a baseline was Matlab’s implementation of the Canny edge detector, with and without hysteresis. For both cases, standard deviation  $\sigma$  was the only parameter to fit, since the thresholding parameters were considered parameters of the Precision-Recall (ROC) curve defined as reference-based evaluation methodology.

We follow the method of [9] to describe the quality of an EDA that produces an edge map  $\mathbf{b}(p)$ , being  $p$  parameters in a one dimensional section  $S$  of the EDA parametric space. Given the EDA, we produce an evaluation curve where each point on the curve is independently computed by first setting the parameters  $p$  of the EDA to produce a binary map and then computing the evaluation measure on such map. When a single performance measure is required or is sufficient, the maximal value of the evaluation measure  $\mathcal{M}$

$$\mathbf{b}_S = \arg \max_{p \in S} \mathcal{M}(\mathbf{b}(p)), \quad (8)$$

is reported as a summary of the detector performance.

#### 4.2. Edge map database

To construct the database, five gradient based EDA were considered: Canny [25], Prewitt [26], Sobel [27], Roberts [28] and Laplacian of Gaussian (LoG) [29], all provided by the Matlab edge function from Matlab’s Image Processing Toolbox.

According to Matlab’s help, Canny EDA has three parameters:  $\sigma$ , Gaussian standard deviation of the derivative filter, and low and high hysteresis thresholding parameters. Edge thinning by non maxima suppression was previously performed to thresholding. The LoG EDA has two parameters:  $\sigma$  (standard deviation of the Gaussian Laplacian filter) and  $T$  (thresholding parameter). Prewitt, Roberts and Sobel EDA are computed by convolving the image with their corresponding gradient operators along the  $x$  and  $y$  direction. Thresholding is later applied to the gradient module. Images are not preprocessed with smoothing or denoising algorithms, since Matlab applies a private function to thinner edges and clean spurious points after thresholding.

For all images, a collection of 100 edge maps were generated by moving each EDA parameters as follows:

- Canny EDA: standard deviation is set at  $\sigma = \sqrt{2}$ , high threshold hysteresis parameter ( $T_h$ ) is (equally spaced) sampled 100 times from zero to one, and the low threshold parameter ( $T_l$ ) is set as  $T_l = 0.4 \times T_h$ .
- Sobel, Prewitt and Roberts EDA: threshold parameter ( $T$ ) is sampled 100 times from 0.004 to 0.396. Edge thinning is turned on.



- LoG EDA: standard deviation is set at  $\sigma = \sqrt{2}$  and the threshold parameter ( $T$ ) is sampled 100 times from 0.0004 to 0.0396.

The final database has 500 edge maps for each real image considered. Moving each EDA threshold from the smallest to the largest value generally produces edge maps with a varying number of featured points. The maximum value of  $\mathcal{C}$  over such EDA outputs selects the edge map with optimal balance between *Equilibrium* and *Information*.

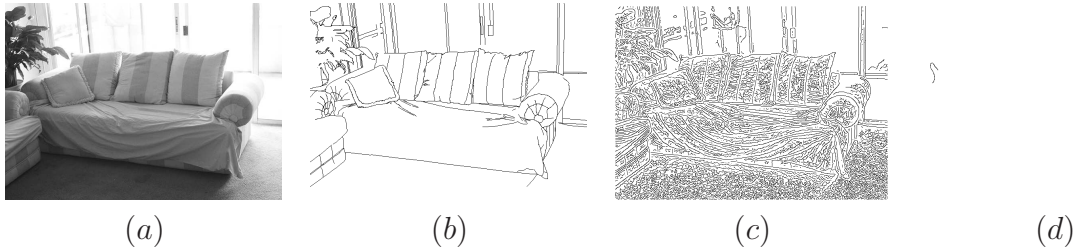


Figure 5: Comparison among GT and extreme edge maps (a) Original image *109*, (b) GT, (c)-(d) Canny's extreme edge maps with  $T_h = 0.01, 0.99$ ;  $T_l = 0.4 \times T_h$ ; and  $\sigma = \sqrt{2}$ .

#### 4.3. First experiment: South Florida database

The South Florida Database is a public database provided by [16] specifically for edge detection assessment. It largely consists of indoor images with little background texture. It includes two collections: one of 50 natural images and other with 10 aerial images. Each of the fifty images of the first collection contains a single object approximately centered in the image and set against a natural background. The second collection has images of man made constructions.

For each of the 60 images, we constructed a database of 500 edge maps and all measures  $\mathcal{E}$ ,  $\mathcal{H}$ ,  $\mathcal{C}$ ,  $\mathcal{Q}_{\mathfrak{B}}$  and PFoM were computed on them, the latest two by using the GT available in the database.

We selected two images for a qualitative performance discussion: image *109*, good quality grayscale indoor image with a central object (Figure 5 (a)) and image *woods*, a good quality outdoors aerial image which depicts several buildings surrounded by woods and country roads (Figure 8). The first image has little texture while the second contains a lot of vegetation (e.g., grass, shrubs, trees), which corresponds to texture in the image. The GT depicts edges only related to object boundary, which do not include the trees present in the image. Overall, this image is a challenge for edge detectors, in particular, for those which only use grayscale information.

In Figure 5, image *109* and its GT are shown along with two extreme edge maps computed with Canny EDA, with  $T_h = 0.01$  and  $T_h = 0.99$ . The first edge map has many texture details transformed in short edges, and the second has almost no edges. The other 98 edge maps are comprised in between these two extreme edge maps.

The evaluation curves, constructed with the values of the  $\mathcal{E}$ ,  $\mathcal{H}$  and  $\mathcal{C}$  over the collection of EDA outputs as a function of the  $T_h$  values, are shown in Figure 6 along with a plot of PFoM and  $\mathcal{Q}_{\mathfrak{B}}$  over the same parameter range. The  $\mathcal{C}$  evaluation curve displays the usual behavior of complexity measures; it shows a peak when both measures are balanced. Qualitative comparisons between best edge maps according to  $\mathcal{C}$  and PFoM

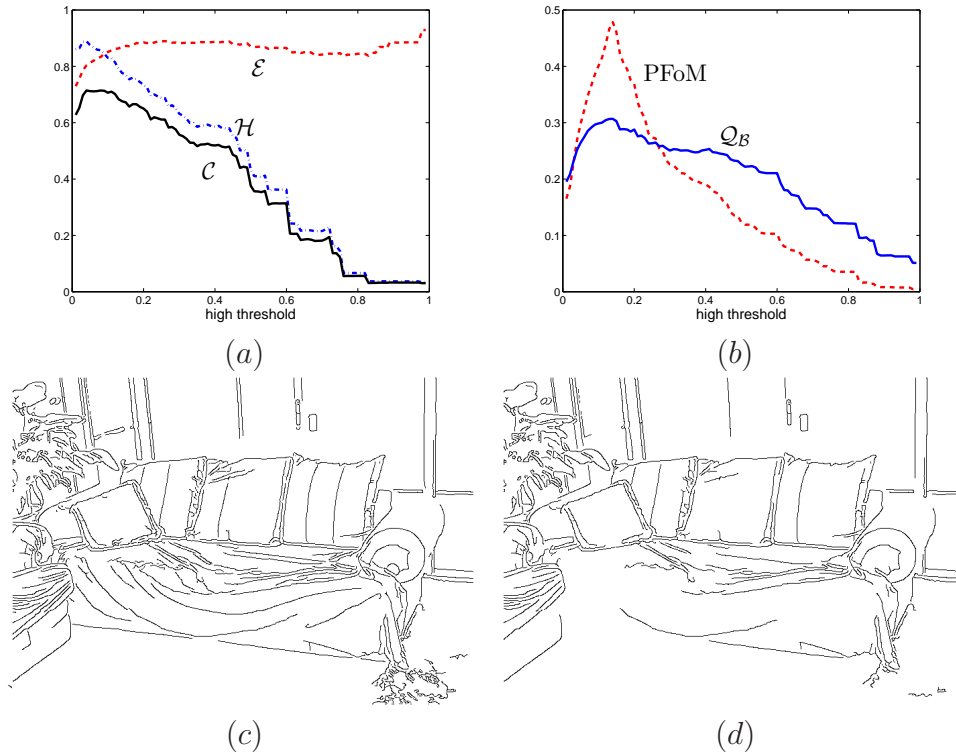


Figure 6: Canny EDA quality curves of image 109. (a) Plot of  $\mathcal{E}$ ,  $\mathcal{H}$  and  $\mathcal{C}$  vs high threshold  $T_h$ , (b) Plot of PFoM and  $\mathcal{Q}_3$  vs  $T_h$ , (c) Best map according to  $\mathcal{C}$  (score 0.714) and (d) Best map according to PFoM (score 0.4784) and  $\mathcal{Q}_3$  (score 0.3068). Canny EDA parameters are high threshold  $T_h=0.08$  and  $0.14$  respectively, low threshold  $T_l = 0.4 \times T_h$  and  $\sigma = \sqrt{2}$ .

are made, see Figure 7. The boundary in the lower part of the coach is missing in the edge map selected by PFoM, (Figure 7 (d)). Our measure selected a more defined edge map, i.e. with more edge points, (Figure 7 (c)), thus showing a more defined contour around the couch. Also, comparing the thresholds value, the  $\mathcal{C}$  measure selected a map with  $T_h = 0.08$  and PFoM a map with higher threshold,  $T_h = 0.14$ . PFoM was reported as a measure with a bias towards false negatives, i.e. it gives higher scores to edge maps with few edges [7]. This account for the missing edge boundary points around the main object in the PFoM edge map.

The second image, *woods*, provides a challenge to all the detectors. The edge maps selected by  $\mathcal{C}$ , PFoM and  $\mathcal{Q}_3$  are shown in Figure 8. Maps are qualitatively different, selected from different quartiles of the parameter range. Reference-based measures select: PFoM to Robert EDA as the best edge detector and  $\mathcal{Q}_3$  to Sobel EDA. Table 1 shows their parameters value and scores. The scores are low, i.e. indicating low agreement between the outputs and GT.

The analysis of the scores given by PFoM and  $\mathcal{Q}_3$  to the edge maps selected by  $\mathcal{C}$ , (Table 2, sixth to seventh column) reveals that the reference-based measures heavily penalize the false positives that are introduced by outlining the woods and country road surrounding the buildings in the image, which are not depicted in the GT. Table 2, third to fifth column, show  $\mathcal{E}$ ,  $\mathcal{H}$  and  $\mathcal{C}$  scores, revealing that the most balanced map related to  $\mathcal{E}$  is given by LoG EDA; the map with most edge entropy, i.e. related to  $\mathcal{H}$ , is given

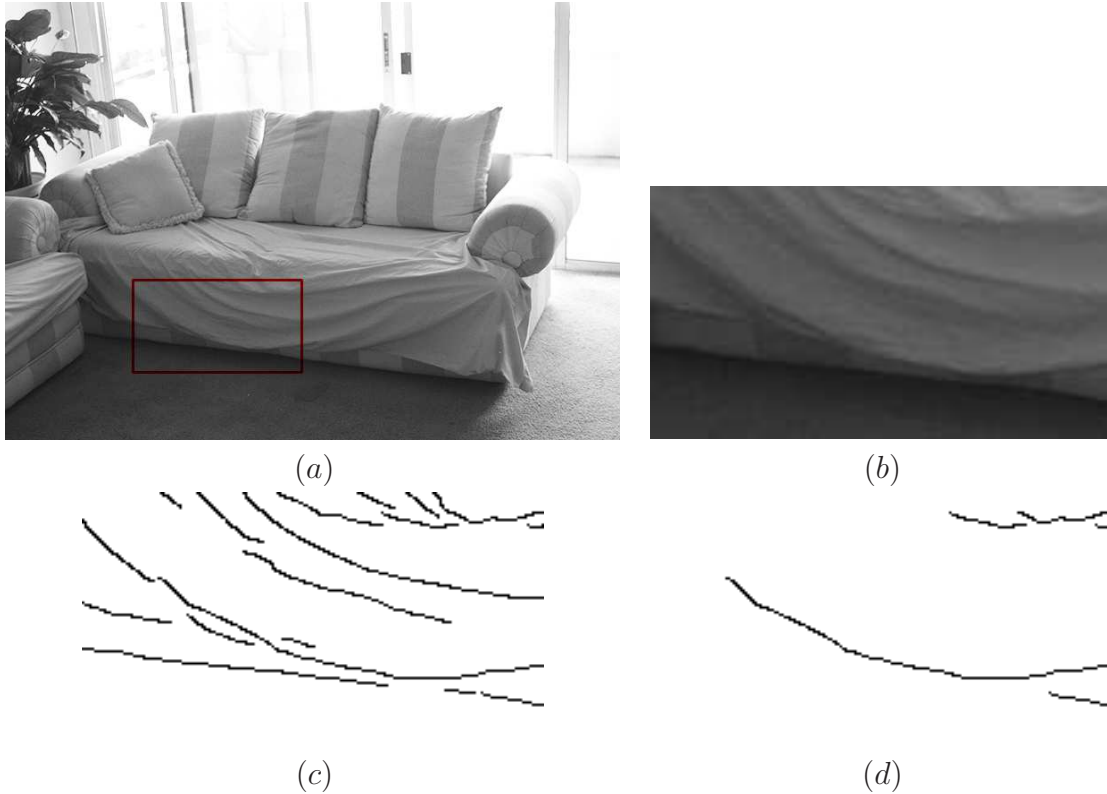


Figure 7: (a) Image 109; (b) Enlarged view of the marked region in (a); (c) Enlarged view of the region shown in (b), extracted from best Canny map according to  $\mathcal{C}$ ; (d) Enlarged view of the region shown in (b), extracted from best Canny map according to PFoM.

by Canny EDA and the one that shows better statistical complexity, i.e. related to  $\mathcal{C}$ , is also Canny EDA. The scores given by PFoM and  $\mathcal{Q}_{\mathfrak{B}}$  to such maps select as the best map the one given by Prewitt EDA. An interesting comparison is given by the scores of  $\mathcal{E}$  and  $\mathcal{Q}_{\mathfrak{B}}$ . The *Equilibrium* index is based on  $\mathcal{Q}_{\mathfrak{B}}$  by replacing the GT with a family of preselected local patterns, sought in the whole image. The provided GT, which does not outline all the objects in the image, misleads the reference-based measures towards lighter maps while the use of pre-defined edge patterns helps preventing such problem.

An enlarged view of the southeast corner of the image *woods* depicting a country road is shown in Figure 9)(a) with its corresponding GT in panel (b). Panel (c) and (d) are Canny edge maps, (e) and (f) LoG edge maps, (g) and (h) Prewitt edge maps, (i) and (j) Sobel edge maps, (k) and (l) Roberts edge maps. The first of each pair was selected by  $\mathcal{C}$  and the second of each pair by PFoM.

In each edge map selected by the reference-based measures, the country road is poorly defined. Instead, every edge map selected by  $\mathcal{C}$ , Figure 9 (c), (e), (g), (i) and (k) have the country road well defined, as well as the vegetation surrounding it.

Finally, we discuss the empirical statistical distribution of the maximum  $\mathcal{C}$  scorings on all EDA maps computed with all South Florida images. Boxplots of such values are shown in Figure 10 along with boxplots of PFoM scores computed on the same edge maps, the ones selected by our  $\mathcal{C}$  measure. We infer from comparison between all  $\mathcal{C}$  empirical

EDA	EDA optimal parameters	PFoM	EDA optimal parameters	$\mathcal{Q}_{\mathfrak{B}}$
Canny	$T_l=0.228$ $T_h=0.57$	0.5082	$T_l=0.264$ $T_h=0.66$	0.3257
LoG	$T=0.0096$	0.4545	$T=0.01$	0.2728
Prewitt	$T=0.0096$	0.5479	$T=0.1$	0.3961
Roberts	$T=0.0096$	<b>0.5565</b>	$T=0.072$	0.3583
Sobel	$T=0.1$	0.5526	$T=0.096$	<b>0.3978</b>

Table 1: Maximum scores of PFoM and  $\mathcal{Q}_{\mathfrak{B}}$  evaluation curves for all EDA, computed over image *woods*. (Maximum scores by column are highlighted in bold typeface.)

EDA	$\mathcal{C}$ -based optimal parameters	$\mathcal{E}$	$\mathcal{H}$	$\mathcal{C}$	PFoM	$\mathcal{Q}_{\mathfrak{B}}$
Canny	$T_l=0.076$ $T_h=0.19$	0.7472	<b>0.9646</b>	<b>0.7208</b>	0.3061	0.2876
LoG	$T=0.0076$	<b>0.7760</b>	0.9201	0.7139	0.3951	0.2654
Prewitt	$T=0.064$	0.7384	0.9262	0.6839	<b>0.4197</b>	<b>0.3787</b>
Roberts	$T=0.0052$	0.6515	0.9368	0.6104	0.3649	0.3348
Sobel	$T=0.064$	0.7326	0.9293	0.6808	0.4137	0.3775

Table 2:  $\mathcal{E}$ ,  $\mathcal{H}$  and  $\mathcal{C}$  scores of best EDA outputs of image *woods*.  $\mathcal{Q}_{\mathfrak{B}}$  and PFoM scores correspond to the best edge map according to  $\mathcal{C}$ . (Maximum scores by column are highlighted in bold typeface.)

distributions that Canny EDA produces slightly better maps than the other detectors. PFoM score differently such maps giving the same moderately low mean (around 0.5 value) to all gradient detectors but LoG EDA. We show examples of such images and best EDA maps in Figure refotras. Each row displays outputs from a different EDA. Last panel of each row shows a plot of the  $\mathcal{C}$  curve as a function of high threshold. The different shapes of the  $\mathcal{C}$  curves can be accounted for the differences in the sampling of each EDA parameter space.

#### 4.4. Second experiment: Image with multiple GT images

Some authors believe that the manual GT approach is essential for performance characterization because most researchers do not regard results on synthetic images as convincing and still wish to see results on real images, see [18] and references therein. Unfortunately, manual GT annotation is dubious, tedious and time-consuming. In addition, different annotators often give different GT or the same annotator can give different GT to the same real image at different times [30]. The use of *consensus* GT for real images avoids both (1) the subjective generation of manual GT for real images and (2) the generation of artificial GT for artificial images, which probably do not faithfully represent the real scenes. On the other hand, the consensus GT allows many real images to be used for performance characterization, [18, 17].

In this experiment, we show that the use of our measure gives results similar to the ones obtained when a pool of GT images are used in the intra-technique and in the inter-technique evaluation problem.

We selected an image from the Berkeley Segmentation Database [30], a benchmark database for boundary detection algorithms that provides images with several hand made

segmentations offered as GT. Thus, the level of detail of the different GT segmentations is diverse, and it represents the human opinion on what the boundary edges of the objects in images are. Besides, edge detection is not the same as boundary detection; boundary maps show only the outline of main objects while edge maps show the whole structure of the image. In Figure 11 five different GT images available for the image *86000* are shown.

All supervised measures depend on the level of detail of the GT, thus any supervised measure computed with GT1 (highly detailed) will give high marks to a more cluttered edge map, but if computed by using GT5 (little detailed) it will certainly give a maximum score to a map with very few edge points.

Unsupervised measures score differently; they search general characteristics in the map, determined in this case by the specific database of edge patterns and the KS statistic. This example aims at exploring the degree of matching of  $\mathcal{C}$  scoring with human observation and supervised measures. Thus we use only the gold standard supervised measure, PFoM, and the gold standard EDA, Canny EDA, to elaborate the example.

We obtained  $\mathcal{C}$  scores for the five GT images and the 100 edge maps outputs of Canny EDA computed with parameters described in the previous subsection. The same 100 Canny edge maps were scored with PFoM, by using all different hand-made GT images and they were scored with  $\mathcal{Q}_{\mathfrak{B}}$  using different collections of GT images. Our reference-based measure  $\mathcal{Q}_{\mathfrak{B}}$  provides a *consensus score* in this framework. In Figure 11 (a), the best map selected by  $\mathcal{C}$  is shown. In panel (b) the optimal edge map selected using PFoM with GT1 image is shown. That map was also selected with the supervised measure  $\mathcal{Q}_{\mathfrak{B}}$  using the collection of all man-made GT images available. In panel (c), the edge map selected by  $\mathcal{Q}_{\mathfrak{B}}$  by using GT2, GT3, GT4 and GT5 is shown. In panel (d), the edge map using PFoM with GT5 is shown.

Visual inspection tells us that the maps selected by PFoM and  $\mathcal{C}$  are almost identical when the GT is the most detailed one (GT1). But the differences are very striking when PFoM is using GT5 (the least detailed one) as GT, i.e. the map selected lost the structure of the building.

In Table 3, the values of  $\mathcal{E}$ ,  $\mathcal{C}$  and  $\mathcal{H}$  over the collection of five GT images are shown. Our  $\mathcal{C}$  measure gives the maximum scoring to the most detailed GT. In this example,

GT	$\mathcal{E}$	$\mathcal{H}$	$\mathcal{C}$
GT1	<b>0.8146</b>	<b>0.8612</b>	<b>0.7015</b>
GT2	0.7730	0.8292	0.6410
GT3	0.7599	0.7852	0.5966
GT4	0.7597	0.7817	0.5939
GT5	0.7778	0.8040	0.6253

Table 3:  $\mathcal{E}$ ,  $\mathcal{H}$  and  $\mathcal{C}$  scores of all GT images available for the image *86000* .(The best results are highlighted in bold typeface.)

three mayor conclusions are drawn:

- By using supervised measures, the degree of details of the GT impacts on the quality of the edge map selected. PFoM selects a better map using a detailed GT than using a less detailed GT. Our reference-based measure  $\mathcal{Q}_{\mathfrak{B}}$  selects edge maps

that are as good as the ones selected by PFoM, and it accommodates the use of a whole collection of GT images to select the best edge map when moving parameters in a fixed range.

- $\mathcal{C}$  selects edge maps that are as good as the ones selected by PFoM at its best (when the GT is detailed enough) but selects better maps than PFoM when the GT is very simple (almost a boundary). The *Equilibrium* index  $\mathcal{E}$  is based on the  $Q_{23}$  measure computed over a rich database of patterns; this operation is better than correlating with a simple (or inaccurate) GT.

## 5. Conclusions

In this paper, new ideas of edge *Equilibrium* and edge *Information* are discussed. They lead to the definition of a new SCM for scoring binary maps. To measure edge *Equilibrium*, a similarity index was defined by projecting the edge map into a family of edge patterns that scores the continuity and width of edges in fixed size windows of the edge map. To measure *Information*, a new *Entropy* index based on the KS statistic was defined. The SCM is the product of the *Equilibrium* and *Entropy* indices and it is effectively used for performance characterization which includes: (i) the specific evaluation of an algorithm (intra-technique process) in order to identify its best parameters, and (ii) the comparison of different algorithms (inter-technique process) in order to classify them according to their quality.

Our experiments were made with common edge detectors that are used by a large number of practitioners. More complex edge detectors aim at specific characteristics in the images, thus the measure should be modified accordingly with a pattern database that accommodates those general characteristics. Active contour methods as applied in [31] are based on the statistical distribution of the noise present in PolSAR images. A measure like ours must carefully be modified to score such EDA outputs, which is the scope of another paper. We are also studying alternative definitions for the *Entropy* index based on edge map histogram functionals that could be tailored to measure the performance of boundary detection algorithms more accurately.

## Acknowledgments

This paper has been partially supported by the Argentinean Grants PICT 2008-00291, and SeCyT-UNC. JM was partially supported by a SGCyT-UNS grad student travel fellowship. JM wants to thanks Famaf-UNC for its hospitality while the preparation of this manuscript. JG was supported by a Conicet graduate student fellowship. The authors wants to thank Prof. Alejandro Frery for enriching discussions that lead to the definition of the measure. All measure related Matlab code was written by the authors and it is available to be downloaded from the Reproducible Research repository of AGF at University of Cordoba.

## References

- [1] I. Abdou, W. Pratt, Quantitative design and evaluation of enhancement/thresholding edge detectors, Proceedings of the IEEE 67 (5) (1979) 753–763.

- [2] L. Kitchen, A. Rosenfeld, Edge evaluation using local edge coherence, *IEEE Transactions on Systems, Man and Cybernetics* 11 (9) (1981) 597–605.
- [3] G. Papari, N. Petkov, Edge and line oriented contour detection: State of the art, *Image and Vision Computing* 29 (2-3) (2011) 79–103.
- [4] W. K. Pratt, *Digital Image Processing*, 4th Edition, Wiley-Interscience, 1978.
- [5] J. Cohen, A coefficient of agreement for nominal scales, *Educational and Psychological Measurement* 20 (1) (1960) 37–46.
- [6] A. J. Baddeley, An error metric for binary images, *Robust Computer Vision: Quality of Vision Algorithms* (1992) 59–78.
- [7] C. Lopez-Molina, B. De Baets, H. Bustince, Quantitative error measures for edge detection, *Pattern Recognition* 46 (24) (2013) 1125–1139.
- [8] W. Jang, C. Kim, SEQM: Edge quality assessment based on structural pixel matching, *IEEE Visual Communications and Image Processing Conference (VCIP)* (2012) 1–6.
- [9] N. Fernandez-García, R. Medina-Carnicer, A. Carmona-Poyato, F. Madrid-Cuevas, M. Prieto-Villegas, Characterization of empirical discrepancy evaluation measures, *Pattern Recognition Letters* 25 (1) (2004) 35–47.
- [10] D. Bryant, D. Bouldin, Evaluation of edge operators using relative and absolute grading, *IEEE Conference on Pattern Recognition and Image Processing* (1979) 138–145.
- [11] Q. Zhu, Efficient evaluations of edge connectivity and width uniformity, *Image and Vision Computing* 14 (1) (1996) 21–34.
- [12] M. Heath, S. Sarkar, T. Sanocki, K. Bowyer, A robust visual method for assessing the relative performance of edge-detection algorithms, *IEEE Transactions on Pattern Analysis and Machine Intelligence (TPAMI)* 19 (12) (1997) 1338–1359.
- [13] J. Bernsen, An objective and subjective evaluation of edge detection methods in images, *Philips Journal of Research* 46 (1991) 57–94.
- [14] S. Nercessian, S. Aghaian, K. Panetta, A new reference-based measure for objective edge map evaluation, *Proceedings SPIE 7351 Mobile Multimedia/Image Processing, Security and Applications* (2009).
- [15] S. Konishi, A. Yuille, J. Coughlan, A statistical approach to multi-scale edge detection, *Image and Vision Computing* 21 (1) (2003) 37–48.
- [16] K. Bowyer, C. Kranenburg, S. Dougherty, Edge detector evaluation using empirical ROC curves, *IEEE Conference on Computer Vision and Pattern Recognition (CVPR)* 1 (1999) 354–359.

- [17] Y. Yitzhaky, E. Peli, A method for objective edge detection evaluation and detector parameter selection, *IEEE Transactions on Pattern Analysis and Machine Intelligence (TPAMI)* 25 (8) (2003) 1027–1033.
- [18] N. Fernandez-García, A. Carmona-Poyato, R. Medina-Carnicer, F. Madrid-Cuevas, Automatic generation of consensus ground truth for the comparison of edge detection techniques, *Image and Vision Computing* 26 (2008) 496–511.
- [19] S. Theodoridis, K. Koutroumbas, *Pattern Recognition*, Elsevier Science, 2008.
- [20] R. López-Ruiz, H. L. Mancini, X. Calbet, A statistical measure of complexity, *Physics Letters A* 209 (5–6) (1995) 321–326.
- [21] J. E. Bresenham, Algorithm for computer control of a digital plotter, *IBM Systems Journal* 4 (1) (1965) 25–30.
- [22] C. E. Shannon, A mathematical theory of communication, *The Bell System Technical Journal* 27 (3) (1948) 379–423.
- [23] A. Justel, D. Peña, R. Zamar, A multivariate Kolmogorov-Smirnov test of goodness of fit, *Statistics & Probability Letters* 35 (3) (1997) 251–259.
- [24] C. Martin, C. Fowlkes, J. Malik, Learning to detect natural image boundaries using local brightness, color and texture cues, *IEEE Transactions on Pattern Analysis and Machine Intelligence (TPAMI)* 26 (5) (2004) 530–549.
- [25] J. Canny, A computational approach to edge detection, *IEEE Transactions on Pattern Analysis and Machine Intelligence (TPAMI)* 8 (6) (1986) 679–698.
- [26] J. M. S. Prewitt, Object enhancement and extraction, B. Lipkin and A. Rosenfeld, Eds. New York: Academic, 1970.
- [27] I. E. Sobel, Camera models and machine perception, Ph.D. thesis, Stanford University, Stanford, CA, USA (1970).
- [28] L. G. Roberts, *Machine Perception of Three-Dimensional Solids*, Outstanding Dissertations in the Computer Sciences, Garland Publishing, New York, 1963.
- [29] D. Marr, E. Hildreth, Theory of Edge Detection, *Proceedings of the Royal Society of London, Series B, Biological Sciences* 207 (1167) (1980) 187–217.
- [30] D. Martin, C. Fowlkes, D. Tal, J. Malik, A database of human segmented natural images and its application to evaluating segmentation algorithms and measuring ecological statistics, *IEEE International Conference on Computer Vision (ICCV)* 2 (2001) 416–423.
- [31] E. Giron, A. Frery, F. Cribari-Neto, Nonparametric edge detection in speckled imagery, *Mathematics and Computers in Simulation* 82 (2012) 2182–2198.



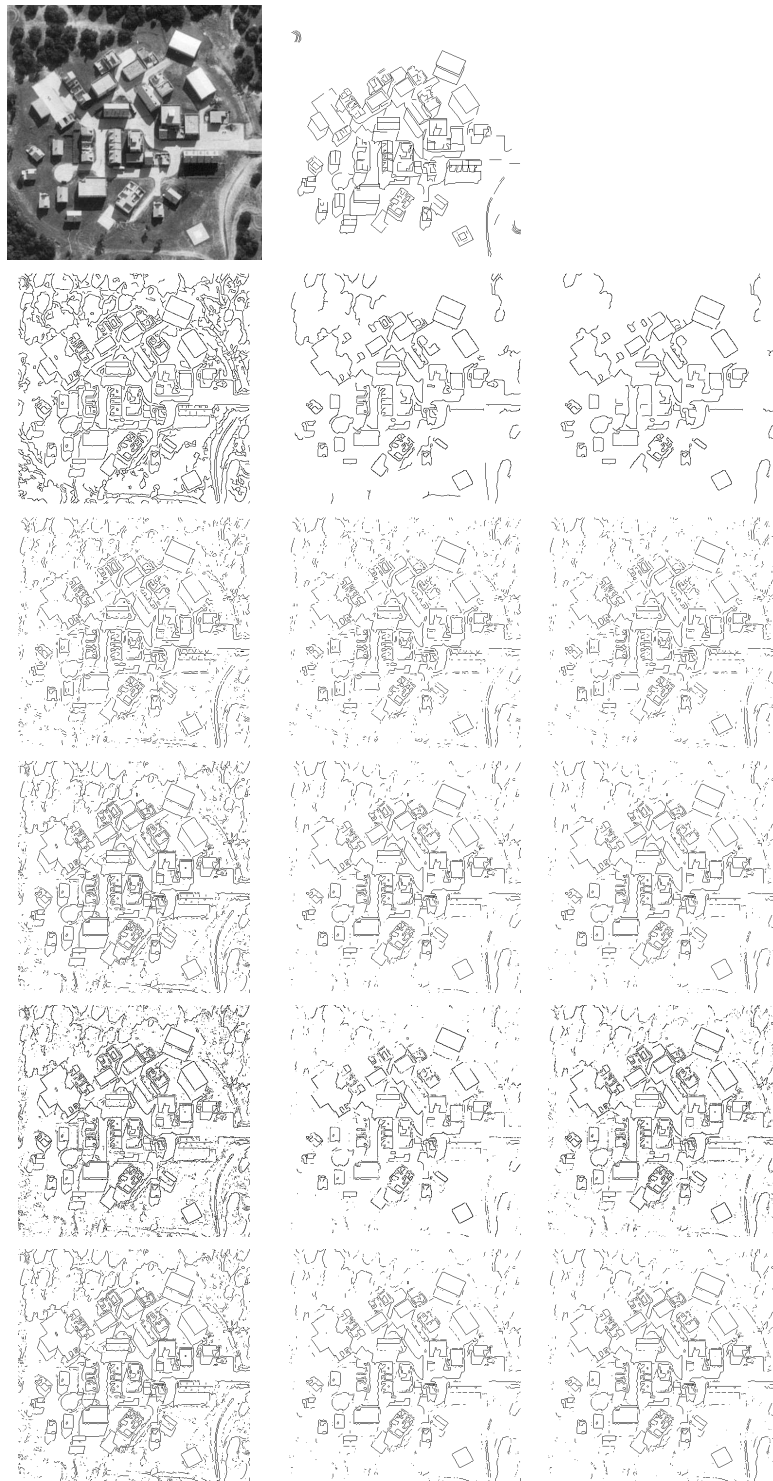


Figure 8: Best EDA map selection according to  $\mathcal{C}$ , PFoM and  $\mathcal{Q}_3$ , from a collection of edge maps of image *woods*, made with different EDA. First row: Original image *woods* and GT. From the second to the last row, each column corresponds to best edge map according to  $\mathcal{C}$ , PFoM and  $\mathcal{Q}_3$  obtained by different EDA: Canny; LoG; Prewitt; Roberts and Sobel, respectively.

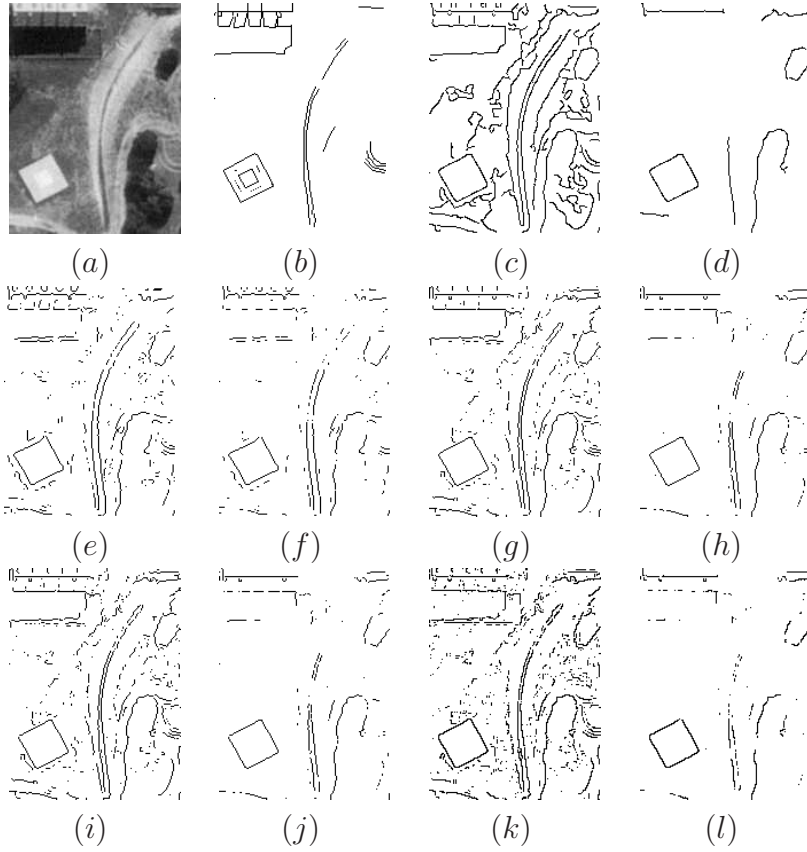


Figure 9: (a) Enlarged view of the southeast corner of the image *woods* depicting a country road. (b) GT from (a). (c) and (d) are Canny edge maps, (e) and (f) LoG edge maps, (g) and (h) Prewitt edge maps, (i) and (j) Sobel edge maps, (k) and (l) Roberts edge maps. The first of each pair was selected by  $\mathcal{C}$  and the second of each pair by PFoM.

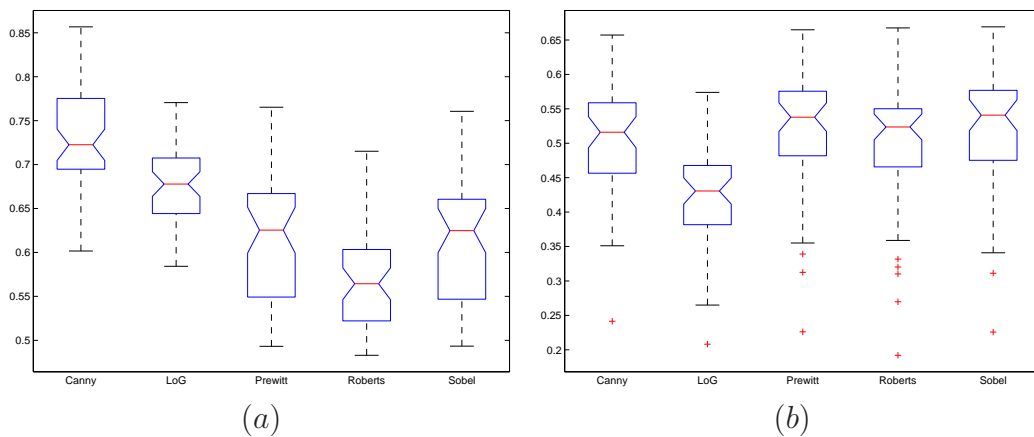


Figure 10: (a) Boxplot of maximum  $\mathcal{C}$  score values, (b) Boxplot of PFoM scores computed on edge maps selected by  $\mathcal{C}$ . Scores are computed over all 50 images of the first collection of South Florida database.

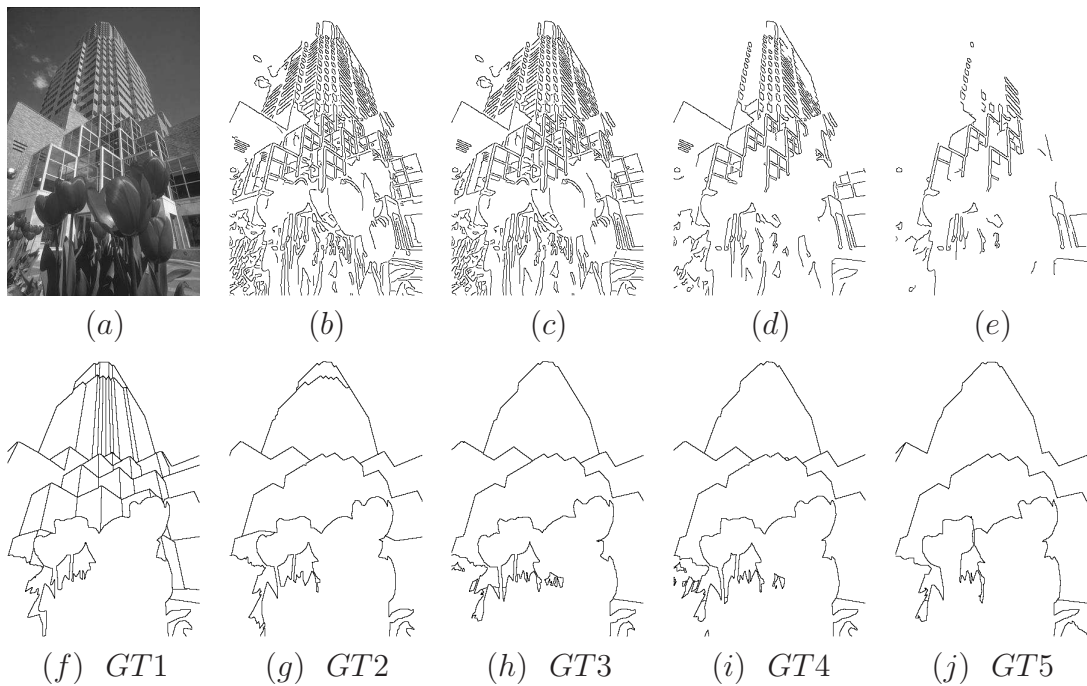


Figure 11: (a) Image 86000; (b) best map selected with measure  $\mathcal{C}$ ; (c) best map selected by PFoM with GT1; (d) best map selected by  $\mathcal{Q}_{23}$  with all GT; (e) best map selected by PFoM with GT3. (f)-(j) are respectively (GT1)-(GT5) GT images from the Berkeley database.

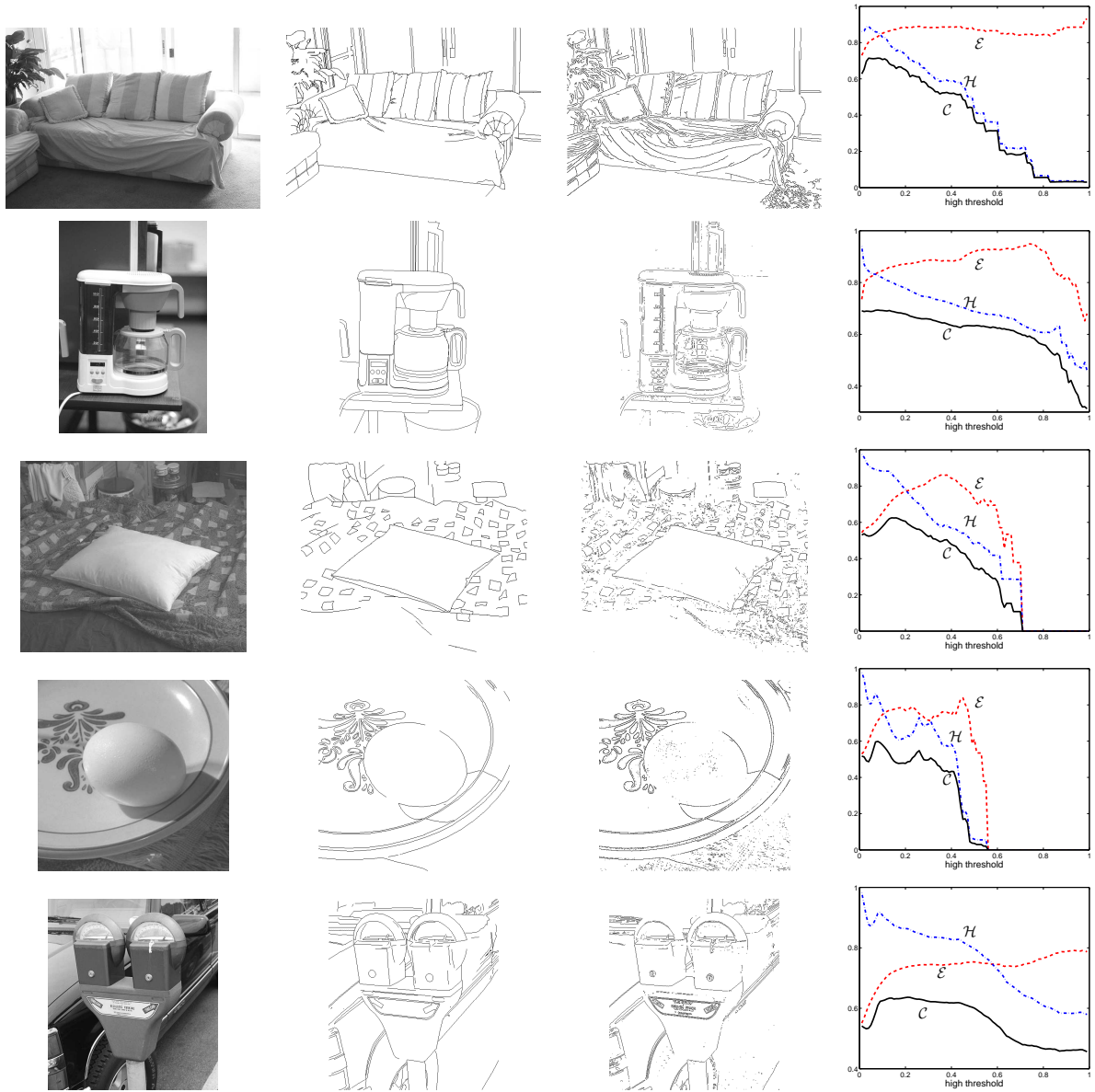


Figure 12: From top to bottom, images and detectors, *109*, Canny; *coffee*, LoG; *218*, Prewitt; *egg*, Roberts; *parkingmeter*, Sobel. The last panel of each row shows plots of the  $\mathcal{C}$  measure vs the threshold values of the corresponding detector.